

Fast3D: Accelerating 3D Multi-modal Large Language Models for Efficient 3D Scene Understanding

Wencan Huang
huangwencan@stu.pku.edu.cn
Wangxuan Institute of Computer
Technology, Peking University
Beijing, China

Daizong Liu
dzliu@stu.pku.edu.cn
Wangxuan Institute of Computer
Technology, Peking University
Beijing, China

Wei Hu*
forhuwei@pku.edu.cn
Wangxuan Institute of Computer
Technology, Peking University
Beijing, China

Abstract

While 3D Multi-modal Large Language Models (MLLMs) demonstrate remarkable scene understanding capabilities, their practical deployment faces critical challenges due to computational inefficiency. The key bottleneck stems from processing excessive object-centric visual tokens required for comprehensive 3D scene representation. Although visual token pruning has shown promise in accelerating 2D MLLMs, its applicability to 3D domains remains largely unexplored due to fundamental disparities in token structures. In this paper, we reveal two critical insights: (1) Significant redundancy exists in object-level 3D token representations, analogous to patch-level redundancy in 2D systems; (2) Global attention patterns exhibit strong predictive power for identifying non-essential tokens in 3D contexts. Building on these observations, we propose Fast3D, a plug-and-play visual token pruning framework for 3D MLLMs featuring two technical innovations: (1) Global Attention Prediction (GAP), where a lightweight neural network learns to predict the global attention distributions of the target model, enabling efficient token importance estimation for precise pruning guidance; (2) Sample-Adaptive visual token Pruning (SAP), which introduces dynamic token budgets through attention-based complexity assessment, automatically adjusting layer-wise pruning ratios based on input characteristics. Both of these two techniques operate without modifying the parameters of the target model. Extensive evaluations across five benchmarks validate the effectiveness of Fast3D, particularly under high visual token pruning ratios. Code is available at <https://github.com/wencan25/Fast3D>.

CCS Concepts

• **Computing methodologies** → **Artificial intelligence; Computer vision; Natural language processing.**

Keywords

Multi-modal Large Language Models, Visual Token Pruning, 3D Scene Understanding

*This paper is supported by the State Key Laboratory of General Artificial Intelligence. Corresponding author: Wei Hu (forhuwei@pku.edu.cn).

Permission to make digital or hard copies of all or part of this work for personal or classroom use is granted without fee provided that copies are not made or distributed for profit or commercial advantage and that copies bear this notice and the full citation on the first page. Copyrights for components of this work owned by others than the author(s) must be honored. Abstracting with credit is permitted. To copy otherwise, or republish, to post on servers or to redistribute to lists, requires prior specific permission and/or a fee. Request permissions from permissions@acm.org.

MM '25, Dublin, Ireland

© 2025 Copyright held by the owner/author(s). Publication rights licensed to ACM.
ACM ISBN XXX-X-XXXX-XXXX-X/XX/XX
<https://doi.org/XX.XXXX/XXXXXXXX.XXXXXXX>

Q: Find the tiny trash can next to the whiteboard. Please share the ID of the object. **A:** Sure, it is <OBJ013>.



Q: What is <OBJ024>? Please describe in detail. **A:** This is an office chair with casters for wheels pulled out from the desk.

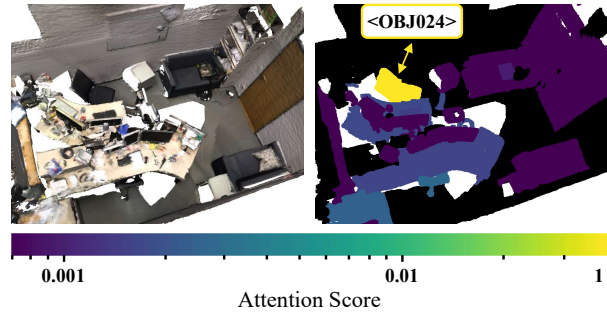


Figure 1: Visualization of the global attention maps aggregated from all layers of Chat-Scene [29], highlighting significant concentration of attention weights on text-relevant 3D objects, which indicates the viability of attention-guided visual token pruning for object-centric 3D MLLMs.

ACM Reference Format:

Wencan Huang, Daizong Liu, and Wei Hu. 2025. Fast3D: Accelerating 3D Multi-modal Large Language Models for Efficient 3D Scene Understanding. In *Proceedings of the 33rd ACM International Conference on Multimedia (MM '25)*, October 27–31, 2025, Dublin, Ireland. ACM, New York, NY, USA, 10 pages. <https://doi.org/XX.XXXX/XXXXXXXX.XXXXXXX>

1 Introduction

The remarkable success of Large Language Models (LLMs) [1, 15, 63] and Multi-modal LLMs (MLLMs) [38, 48, 86] has sparked growing interest in extending their applications to the 3D domain for embodied intelligent agents. By encoding object-centric 3D representations and mapping these features onto the latent semantic space of LLMs as visual tokens, 3D MLLMs [29, 31, 37, 77] have demonstrated exceptional scene understanding capabilities in core 3D vision-language tasks such as referred object grounding [7, 79], dense scene captioning [14], and situated question answering [3, 50], leveraging a unified multi-modal sequence modeling paradigm.

However, this paradigm often suffers from substantial computational overhead due to the reliance on an excessive number of visual tokens, limiting practical deployment. For instance, Chat-Scene [29] adopts 300 visual tokens for a 100-object scene through tripartite encoding, which requires over 5 times the token consumption compared to its text-only inference on ScanQA [3]. More recent approaches [77] resort to integrating auxiliary visual tokens such as semantic relationships between objects to enhance performance, inflating the visual token count to 800 per scene, which further exacerbates the already high computation of 3D MLLMs.

Training-free visual token pruning approaches [4, 9, 60, 78, 81] have emerged as a compelling solution for accelerating 2D MLLMs. Previous methods [9, 78] typically utilize partial model information (e.g., attention maps from early layers) to eliminate less critical image tokens. Recent advances like SGL [81] demonstrate enhanced efficiency by leveraging global attention patterns from compact MLLMs to guide token pruning in larger counterparts. While these techniques have significantly optimized 2D MLLMs, their applicability to 3D MLLMs remains largely unexplored due to fundamental differences in token structures. Unlike the inherently redundant patch-level tokens in 2D vision systems, the visual tokens in representative 3D MLLMs are object-centric with explicit spatial-semantic grounding. This structural distinction raises critical questions: *Does conventional token redundancy persist in 3D representations? Can attention-guided pruning maintain effectiveness when applied to discrete object tokens?* To investigate these questions, we conduct a preliminary study by visualizing the global attention distributions in Chat-Scene [29]. As shown in Figure 1, we observe that the aggregated attention maps accurately concentrate on a few text-relevant objects, demonstrating significant redundancy even in structured 3D representations. Our empirical evidence reveals two key findings: (1) *Object-centric architectures do not inherently eliminate token redundancy, and (2) Global attention patterns aggregated from all layers of the target model are superior pruning indicators for 3D MLLMs.*

However, retrieving attention maps from all layers necessitates full-model inference, making it infeasible for practical deployment. To mitigate this, existing approaches like SGL [81] attempt to leverage the aggregated attention maps from a smaller MLLM to guide pruning in a larger one. But this method suffers from two fundamental limitations. First, the smaller model is trained independently without joint optimization, leading to potential inconsistencies in attention distributions. Second, the smaller model in SGL, with its 2 billion parameters, is not sufficiently lightweight, introducing non-negligible computational overhead. These issues are further compounded in resource-constrained 3D domains, where such small-scale yet capable MLLMs may not be readily available. Therefore, how to accurately identify critical visual tokens in 3D MLLMs with minimal computation remains an open challenge.

To address this challenge, we present **Fast3D**, a plug-and-play visual token pruning framework to reduce the inference cost of 3D MLLMs with two technical innovations. First, we develop a *Global Attention Prediction (GAP)* mechanism that systematically identifies essential 3D visual tokens through attention distillation. Specifically, we propose training a lightweight GAP network to predict the oracle attention map aggregated across all layers of 3D MLLMs capturing three crucial interactions: the self-attention of

vision tokens and their cross-modal interactions with prompt and generated text. The network adopts an encoder-decoder architecture with early fusion of three complementary embeddings – visual semantics, spatial coordinates, and object identifiers – resulting in reduced computational cost and improved prediction accuracy. During inference, the predicted attention maps provide a precise guidance for pruning less important visual tokens in 3D MLLMs.

While efficient token importance estimation is essential, when and how to prune visual tokens remains a key challenge. Existing pruning strategies [9, 74, 81] typically rely on static, empirically set pruning ratios, applying uniform token budgets across all inputs regardless of task complexity. Such rigidity ignores the inherent diversity in visual-linguistic difficulty across samples. To overcome this limitation, we introduce *Sample-Adaptive visual token Pruning (SAP)*, which dynamically adjusts token budgets based on attention-driven complexity assessment. SAP estimates the per-sample difficulty and adaptively allocates pruning ratios at each transformer layer, allowing the model to retain more tokens for complex instructions and fewer for simpler ones. To further enhance deployment efficiency, we perform an offline binary search to optimize the pruning configuration under fixed computational budgets, achieving improved overall accuracy-efficiency trade-offs.

In summary, our main contributions are threefold:

- We reveal the substantial redundancy of visual tokens in object-centric 3D MLLMs via investigating their global attention patterns, indicating that a great number of visual tokens can be discarded during inference with negligible performance drop.
- We propose **Fast3D**, a plug-and-play visual token pruning framework tailored for 3D MLLMs featuring two novel components: (1) *Global Attention Prediction (GAP)*, where we train a lightweight neural network for efficient token importance estimation; (2) *Sample-Adaptive visual token Pruning (SAP)*, which dynamically adjusts token budgets based on input complexity to achieve improved overall accuracy-efficiency trade-offs.
- We demonstrate the superiority of Fast3D through comprehensive evaluations across five 3D vision-language tasks, enabling up to 90% visual token reduction in 3D MLLMs like Chat-Scene while maintaining over 96.8% of original performance, achieving significantly higher efficiency for 3D scene understanding.

2 Related Work

2.1 3D Multi-modal Large Language Models

The prevalence of Large Language Models (LLMs) [15, 63] and Multi-modal LLMs (MLLMs) [46–48, 71, 86] has sparked growing interest in extending their reasoning capabilities to the 3D domain, leading to the emergence of 3D MLLMs for point cloud object understanding [16, 22, 23, 55, 56, 62, 72] and 3D scene understanding [11, 13, 21, 27–29, 33, 34, 44, 45, 57, 69, 76]. For 3D scene-level MLLMs, the pioneering work [28] renders 3D environments into multi-view images, leveraging pre-trained 2D MLLMs for 3D comprehension. Subsequent works directly project scene-level point clouds into the embedding space of LLMs via MLPs [27] or Qformers [11] for enhanced structural preservation. Recent models such as Chat-3D [30, 70], Chat-Scene [29], LEO [31], Robin3D [37], and 3DGraphLLM [77] predominantly adopt object-centric architectures to capture intricate spatial-semantic relationships. For

example, Chat-3D v2 [30] employs off-the-shelf 3D detectors [59] to extract per-object spatial features and introduces object identifiers for precise object referencing and grounding. More recent approaches further enhance performance by integrating auxiliary visual tokens, such as multi-view 2D representations [29] and semantic relationships between objects [77]. However, the increasing number of visual tokens also greatly exacerbates the already high computational costs of 3D MLLMs. In this paper, we address the token overhead with a plug-and-play visual token pruning framework, enabling more efficient 3D scene understanding.

2.2 Visual Token Compression

Visual token compression has been widely explored in transformer-based vision models, such as ViTs [2, 64], aimed at reducing computational overhead through token pruning [5, 20, 42, 58, 68], merging [4, 10, 36, 61], and skipping [24, 26, 51, 82, 83] techniques. In the context of MLLMs, prior works have explored compression strategies from both efficient projector design [6, 17, 18, 40, 41] and dynamic token reduction [8, 52, 73, 75] perspectives, seeking to eliminate redundant visual tokens while maintaining model performance. However, these methods often require additional fine-tuning of the base model. In contrast, more recent training-free approaches [9, 25, 32, 35, 39, 43, 60, 67, 74, 78, 80, 81, 84, 87] can be deployed directly on pre-trained MLLMs without requiring parameter updates, offering a more practical solution for improving efficiency. For instance, methods like LLaVA-PruMerge [60] and VTC-CLS [67] merge tokens within the visual encoder before feeding them into the LLM. Other approaches, such as FastV [9] and SparseVlm [78], prune inattentive visual tokens in specific LLM layers based on attention maps between visual and instruction tokens, utilizing manually designed reduction strategies. Meanwhile, techniques like FitPrune [74] attempt to automatically determine the optimal pruning recipe under predefined computation budgets. However, these methods can struggle to accurately identify essential visual tokens due to their reliance on partial information from early LLM layers. Recently, SGL [81] shows that the global attention map aggregated from all layers of small MLLMs can provide better guidance for pruning in larger MLLMs. Despite these advancements, limited research explores the effectiveness of visual token pruning for object-centric architectures like 3D MLLMs.

3 Methodology

We begin by providing the preliminaries on typical scene-level 3D MLLMs in Section 3.1. Subsequently, we detail Fast3D, the proposed plug-and-play visual token pruning framework, which incorporates two innovative techniques. Specifically, Section 3.2 details the Global Attention Prediction (GAP) mechanism for efficient token importance estimation, while Section 3.3 introduces the Sample-Adaptive visual token Pruning (SAP) strategy.

3.1 Preliminary

In this study, we use Chat-Scene [29], a state-of-the-art 3D MLLM with an exemplar object-centric architecture for 3D scene understanding, as the base model for demonstrating our proposed inference acceleration framework. Chat-Scene features three core components: 1) Visual Encoding: This module processes raw 3D scenes

into structured object-level representations through tripartite encoding. First, a pre-trained Mask3D detector [59] decomposes the scene into n object proposals. Then, each object receives a unique object identifier embedding $\mathbf{E}_i^o \in \mathbb{R}^d$ added to the language model vocabulary, the geometric embedding $\mathbf{E}_i^p \in \mathbb{R}^{d_p}$ from point clouds via Uni3D [85], and the visual embedding $\mathbf{E}_i^v \in \mathbb{R}^{d_v}$ extracted from multi-view images using DINOv2 [53]. 2) Visual Projection: Object embeddings are mapped to the LLM’s latent space as visual tokens. For the i -th object, its visual tokens are represented as $\mathbf{V}_i^o = \mathbf{E}_i^o$, $\mathbf{V}_i^p = f_p(\mathbf{E}_i^p)$, and $\mathbf{V}_i^v = f_v(\mathbf{E}_i^v)$, where $f_p(\cdot)$ and $f_v(\cdot)$ are fully connected projectors. 3) Multi-modal Language Modeling: The LLM takes visual and textual tokens as input, and generates the next text token in an autoregressive manner. At inference step i , the input sequence is:

$$\mathbf{X}^i = [\mathbf{V}, \mathbf{T}, \mathbf{G}^i] \in \mathbb{R}^{(3n+m+i) \times d}, \quad (1)$$

$$\mathbf{V} = \parallel_{k=1}^n [\mathbf{V}_k^o, \mathbf{V}_k^p, \mathbf{V}_k^v] \in \mathbb{R}^{3n \times d}, \quad (2)$$

where $\mathbf{V} \in \mathbb{R}^{3n \times d}$ denotes the concatenated visual tokens, $\mathbf{T} \in \mathbb{R}^{m \times d}$ is the textual prompt tokens, and \mathbf{G}^i is the previous generated text tokens. With tripartite encoding, we usually have $3n \gg m$, especially for complex 3D scenes with dense objects.

3.2 Global Attention Prediction

The computational burden of processing excessive visual tokens significantly impedes 3D MLLM inference efficiency. While attention-guided visual token pruning [9, 81] shows promise in accelerating 2D MLLMs, its adaptation to object-centric 3D MLLMs remains unexplored. Our empirical analysis demonstrates that *global attention patterns aggregated from all layers of the target model retain the viability as superior pruning indicators in 3D domains* (Table 2). However, deriving these oracle attention maps requires full-model inference, creating a practical deployment paradox. Existing approximations like SGL [81] that employs smaller MLLMs to guide pruning in larger models exhibit fundamental limitations: 1) Attention pattern mismatch due to independent model training without joint optimization, 2) Non-negligible computational overhead from insufficiently compact proxy models, and 3) Scarcity of pre-trained small MLLMs in 3D domains. This presents a critical challenge:

How to accurately identify essential visual tokens in 3D MLLMs with minimal computation?

We introduce Global Attention Prediction (GAP) (Figure 2a-b) as a novel solution: *training a lightweight GAP network to predict the aggregated attention map of the target 3D MLLM as a precise and efficient pruning guidance.*

3.2.1 Global Attention Aggregation. In order to train the GAP network, we extract ground-truth global attention maps from the frozen target 3D MLLM, as shown in Figure 2b. Given an input training sequence \mathbf{X} composed of $3n$ visual tokens, m prompt tokens, and t generated tokens, let $\mathbf{A}^{(l,h)} \in \mathbb{R}^{(3n+m+t) \times (3n+m+t)}$ denote the attention matrix at layer l and head h . The aggregated attention map is computed via uniform averaging across all L layers and H heads: $\mathbf{A} = \frac{1}{LH} \sum_{l=1}^L \sum_{h=1}^H \mathbf{A}^{(l,h)} \in \mathbb{R}^{(3n+m+t) \times (3n+m+t)}$. We then aggregate the attention scores of visual tokens received from other tokens to form a global object-centric attention map through three complementary mechanisms:

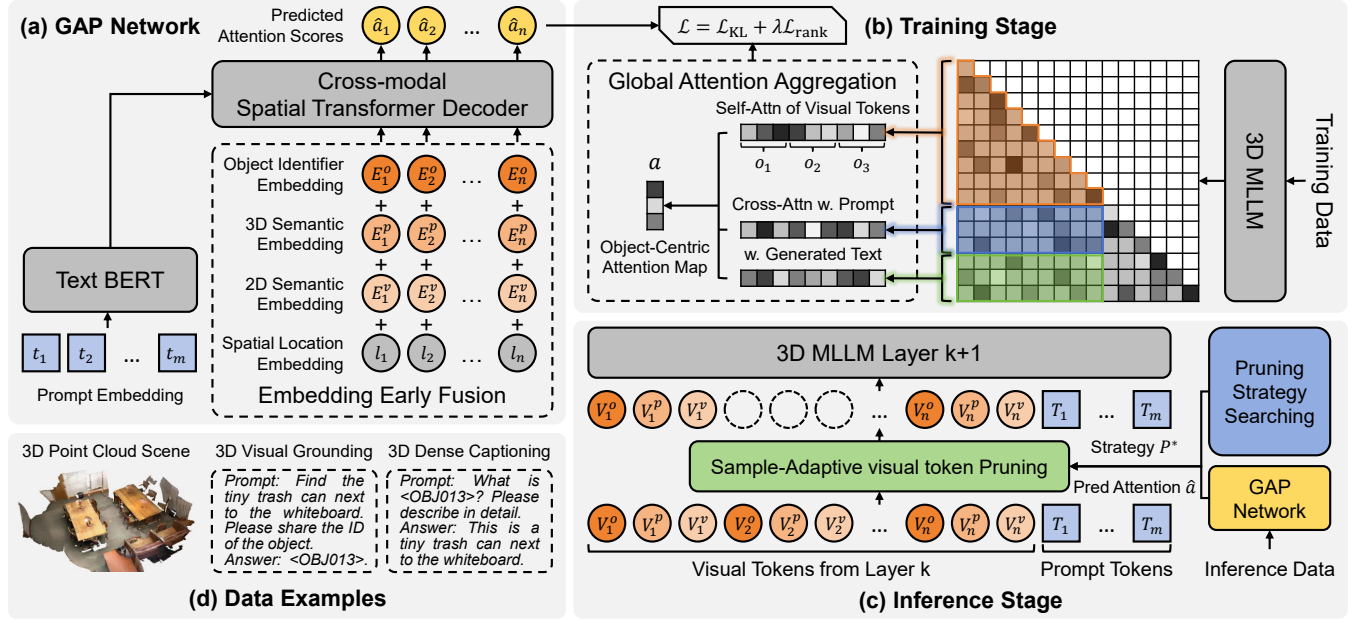


Figure 2: Framework of Fast3D. (a) The GAP network learns to predict the aggregated attention maps of the target 3D MLLM, providing efficient and accurate guidance for visual token pruning. (b) During training, we construct the ground-truth object-centric attention map by aggregating attention scores of visual tokens received from other tokens across all heads and layers of the target model. (c) At inference stage, we employ an optimized pruning strategy to eliminate less-important visual tokens sample-adaptively based on GAP predictions. (d) Data examples of diverse 3D scene understanding tasks.

Self-Attention of Visual Tokens. Let $A_{\text{self}} \in \mathbb{R}^{3n \times 3n}$ denote the top-left submatrix of A , where each entry $A_{\text{self}}(i, j)$ reflects the dependency between visual tokens V_i and V_j . Considering the causal attention structure, we compute visual token importance $a_{\text{self}} \in \mathbb{R}^{3n}$ using masked column-wise averaging:

$$a_{\text{self}}(j) = \frac{1}{3n - j + 1} \sum_{i=1}^{3n} M_{\text{causal}}(i, j) \cdot A_{\text{self}}(i, j), \quad (3)$$

where M_{causal} is a lower-triangular mask ensuring visual token V_i only attends to preceding tokens $V_{j \leq i}$. High-value entries in a_{self} indicate geometrically or semantically correlated objects that the 3D MLLM inherently prioritizes for visual reasoning.

Cross-Attention with Prompt. For m prompt tokens, let $A_{\text{prompt}} \in \mathbb{R}^{m \times 3n}$ be the cross-attention sub-matrix. We derive prompt-aware token importance $a_{\text{prompt}} \in \mathbb{R}^{3n}$ through average pooling:

$$a_{\text{prompt}}(j) = \frac{1}{m} \sum_{i=1}^m A_{\text{prompt}}(i, j), \quad (4)$$

which highlights visual tokens most responsive to task-specific linguistic cues, ensuring instruction-aligned feature preservation.

Cross-Attention with Generated Text. For t generated text tokens with teacher forcing, let $A_{\text{text}} \in \mathbb{R}^{t \times 3n}$ denote the bottom-left block. We compute generation-aware importance $a_{\text{text}} \in \mathbb{R}^{3n}$ with a confidence-weighted average:

$$a_{\text{text}}(j) = \frac{1}{\sum_{i=1}^t s^{(i)}} \sum_{i=1}^t s^{(i)} \cdot A_{\text{text}}(i, j), \quad (5)$$

where $s^{(i)}$ represents the softmax probability of the next generated token at the i -th step. This emphasizes visual tokens consistently supporting high-confidence text generation.

The global attention map $a_{\text{global}} \in \mathbb{R}^{3n}$ is obtained through element-wise summation of the three components: $a_{\text{global}} = a_{\text{self}} + a_{\text{prompt}} + a_{\text{text}}$. This comprehensive assessment is further averaged across the object dimension and normalized to get the final object-centric attention map $a \in [0, 1]^n$, which serves as the training target for our GAP network.

3.2.2 Lightweight GAP Network Learning. The GAP network learns to predict aggregated attention maps of the target 3D MLLM to facilitate visual token pruning. As shown in Figure 2a, the network's input closely mirrors that of the target model, encompassing textual prompts and structured object-centric visual embeddings encoding the 3D scene. The network is designed to achieve precise and computationally efficient attention prediction:

Embedding Early Fusion. For each object o_i , we enhance spatial awareness by encoding its center coordinates $c_i \in \mathbb{R}^3$ and bounding box dimensions $z_i \in \mathbb{R}^3$ via linear projection to obtain the spatial location embedding as $l_i = W_l[c_i; z_i] \in \mathbb{R}^d$. An early fusion strategy is adopted to integrate visual embeddings from different sources. We first fuse 3D and 2D semantic embeddings with a multi-layer perceptron as $E_i^s = \text{MLP}([E_i^p; E_i^v])$. Then, the object identifiers, fused semantic embeddings, and spatial location features are added together as the final fused object-centric embeddings: $F_i = E_i^o + E_i^s + l_i$. This compressed fusion scheme reduces the input sequence length while preserving multi-modal correlations.

Encoder-Decoder Architecture. The GAP network adopts a light-weight encoder-decoder architecture. We finetune a pre-trained BERT [19] to encode the prompt into a sequence of text features. A spatial transformer decoder [12] is then applied to learn cross-modal correlations between the text and object modality features. Each transformer layer consists of a spatial self-attention module, a cross-attention module and a feed-forward neural network. The spatial self-attention mechanism improves the understanding of spatial relations among objects referenced in the instruction. The final layer outputs attention logits normalized via softmax to produce predicted object-centric attention distribution $\hat{\mathbf{a}}$.

Multi-Objective Optimization. To optimize the GAP network, we employ a multi-objective loss function that simultaneously enforces attention fidelity and rank consistency, which are critical for effective downstream pruning:

$$\mathcal{L} = \underbrace{\text{KL}(\mathbf{a} \parallel \hat{\mathbf{a}})}_{\text{Attention Fidelity}} + \lambda \underbrace{\sum_{i,j} \mathbf{1}(a_i > a_j) \cdot \max(0, \hat{a}_j - \hat{a}_i + \delta)}_{\text{Rank Consistency}}, \quad (6)$$

where $\mathbf{a} \in [0, 1]^n$ represents the ground-truth attention map. The first term, based on Kullback-Leibler (KL) divergence, ensures precise attention distribution alignment while the second term explicitly enforces pairwise ranking consistency by penalizing violations in the relative ordering of attention scores. To prevent over-smoothing and improve discriminative capability, we apply temperature sharpening to \mathbf{a} before KL computation.

3.3 Sample-Adaptive Visual Token Pruning

To improve the efficiency of the target 3D MLLM, we prune less important visual tokens based on the estimated token importance score $\hat{\mathbf{a}}$. Existing pruning strategies can be categorized into two types: 1) Uniform compression maintaining fixed retention ratios from an intermediate layer onward, such as FastV [9] and SGL [81]; 2) Preserving different proportions of the most important visual tokens at each layer of the target model, exemplified by FitPrune [74]. These methods rigidly predefine pruning ratios through empirical validation or automated search, maintaining constant per-sample token budgets regardless of input characteristics during inference. However, this static approach fundamentally conflicts with *the intrinsic variance in visual-linguistic complexity across input samples – simpler instructions require fewer discriminative tokens while complex tasks demand richer representations*. To resolve this limitation, we propose Sample-Adaptive visual token Pruning (SAP), which dynamically adjusts layer-wise token budgets based on input complexity for improved efficiency.

Specifically, we hypothesize that the concentration degree of the predicted attention map $\hat{\mathbf{a}} \in [0, 1]^n$ correlates with sample difficulty: concentrated distributions indicate easier samples with clearer identification of key tokens, while uniform distributions suggest harder samples with obscure token significance. To operationalize this, we introduce layer-wise total attention thresholds θ_k to dynamically determine token retention counts, replacing fixed pruning ratios. Given an inference sample x with predicted attention scores $\hat{\mathbf{a}}^{(x)}$ ranked in descending order via permutation π , the number of retained visual tokens $r_k^{(x)}$ at layer k (where each 3D MLLM triplet $\{\mathbf{V}_i^o, \mathbf{V}_i^p, \mathbf{V}_i^v\}$ is treated as a single token intuitively)

Algorithm 1 Pruning Strategy Searching

Require: model \mathcal{G} , data batch \mathcal{X} , predicted attention $\hat{\mathbf{a}}$, target FLOPs budget δ and binary search parameters $\epsilon, \alpha_{\min}, \alpha_{\max}$

- 1: Initialize $\alpha_{\text{low}} = \alpha_{\min}, \alpha_{\text{high}} = \alpha_{\max}$
- 2: Initialize $\mathbf{P}^0 = [\theta_1^0, \theta_2^0, \dots, \theta_L^0]$ manually or via FitPrune [74] as $\theta_k^0 = \max_{x \in \mathcal{X}} \sum_{i=1}^{r_k^0} \hat{a}_{\pi(i)}^{(x)}$, where r_k^0 denotes the obtained static token retention count at layer k
- 3: **while** $\alpha_{\text{high}} - \alpha_{\text{low}} > \epsilon$ **do**
- 4: $\alpha_{\text{mid}} \leftarrow (\alpha_{\text{low}} + \alpha_{\text{high}})/2$
- 5: $C_{\text{mid}} \leftarrow \sum_{x \in \mathcal{X}} \Phi(\mathcal{G}, \mathbf{P}(\alpha_{\text{mid}}), \hat{\mathbf{a}}^{(x)}, x)$
- 6: **if** $C_{\text{mid}} \leq \delta$ **then** $\alpha_{\text{low}} \leftarrow \alpha_{\text{mid}}$ **else** $\alpha_{\text{high}} \leftarrow \alpha_{\text{mid}}$
- 7: **end while**
- 8: $\alpha^* \leftarrow \alpha_{\text{low}}$
- 9: **return** Pruning strategy $\mathbf{P}^* = [\alpha^* \theta_1^0, \alpha^* \theta_2^0, \dots, \alpha^* \theta_L^0]$

can be calculated as:

$$r_k^{(x)} = \max \left\{ j \in \{1, 2, \dots, n\} \mid \sum_{i=1}^j \hat{a}_{\pi(i)}^{(x)} \leq \theta_k \right\}. \quad (7)$$

This formulation ensures ordered token retention based on predicted attention scores while enforcing cumulative threshold constraints. The dynamic computation of $\hat{\mathbf{a}}$ through the GAP network enables sample-specific retention ratios, achieving adaptive pruning at the instance level.

Our SAP framework is fully parameterized by $\mathbf{P} = [\theta_1, \theta_2, \dots, \theta_L]$, representing the total attention thresholds for each layer. To determine an optimal pruning strategy under a given computational budget, we further introduce **Pruning Strategy Searching** (Algorithm 1). Specifically, we define the pruning strategy \mathbf{P} as a scaled variant of a set of predefined baseline parameters $\mathbf{P}^0 = [\theta_1^0, \theta_2^0, \dots, \theta_L^0]$, i.e., $\mathbf{P}(\alpha) = \alpha \mathbf{P}^0$, where \mathbf{P}^0 can be initialized manually or based on the FitPrune [74] algorithm. Given a small batch of validation data \mathcal{X} , the total computation overhead of the model \mathcal{G} can be expressed as: $f(\alpha) = \sum_{x \in \mathcal{X}} \Phi(\mathcal{G}, \mathbf{P}(\alpha), \hat{\mathbf{a}}^{(x)}, x)$. Since this cost function increases monotonically, we perform binary search to find the maximum α^* such that $f(\alpha) \leq \delta$, where δ denotes the predefined FLOPs computational budget. The optimal pruning strategy is then obtained as $\mathbf{P}^* = \alpha^* \mathbf{P}^0$.

4 Experiment

4.1 Experimental Setup

Datasets and Metrics. We conduct experiments on five 3D vision-language datasets: ScanRefer [7] for single-object visual grounding, Multi3DRefer [79] for multi-object visual grounding, Scan2Cap [14] for dense captioning, and both ScanQA [3] and SQA3D [50] for visual question answering. All experiments on these datasets follow the default settings and metrics. For ScanRefer [7], we evaluate thresholded accuracy with Acc@0.25 and Acc@0.5, where predictions are deemed positive if they exhibit higher Intersection over Union (IoU) with the ground truths than the thresholds. Multi3DRefer [79] is assessed using the F1 score at IoU thresholds of 0.25 and 0.5. For Scan2Cap [14], we adopt CIDEr@0.5 and BLEU-4@0.5, integrating captioning metrics with the IoU scores.

Table 1: Performance comparison with previous visual token compression methods. “Pruning Ratio” denotes the average ratio of pruned visual tokens. “Score Ratio” is obtained by calculating the average ratio of each score relative to Baseline.

	Method	Pruning Ratio	ScanRefer		Multi3DRefer		Scan2Cap		ScanQA		SQA3D		Score Ratio
			Acc@0.25	Acc@0.5	F1@0.25	F1@0.5	C@0.5	B-4@0.5	C	B-4	EM	EM-R	
Chat-Scene [29]	Baseline	0%	56.21	50.42	58.14	53.24	76.35	35.86	84.23	13.57	53.98	56.80	100.00%
	Random Pruning	35%	36.06	31.54	40.85	36.62	72.77	34.90	81.61	12.75	52.74	55.28	84.42%
		65%	14.67	12.51	19.92	18.04	31.14	26.61	76.42	12.28	51.02	53.41	60.38%
		90%	3.50	2.83	9.59	9.25	21.74	23.36	67.94	10.65	48.48	50.99	47.80%
	ToMe [4]	35%	50.43	45.39	51.95	47.70	73.43	35.76	83.46	13.39	52.64	55.12	94.69%
		65%	26.86	24.48	30.99	28.98	45.10	29.11	83.28	13.03	52.22	54.81	73.24%
		90%	3.72	2.96	9.63	9.28	21.45	23.05	67.03	10.51	47.83	50.31	47.31%
	FastV [9]	35%	55.40	49.86	57.39	52.69	75.94	35.89	84.49	12.90	54.22	56.77	99.04%
		65%	29.13	26.55	33.61	31.44	47.42	30.60	84.96	13.40	53.27	55.91	76.55%
		90%	3.92	3.23	9.20	8.91	18.65	21.88	65.28	10.31	48.16	50.76	46.34%
	GAP (Ours)	35%	56.61	51.02	58.33	53.52	75.83	35.56	85.13	13.06	53.95	56.49	99.79%
		65%	56.47	50.79	58.46	53.86	73.24	34.77	85.23	13.00	53.55	56.25	99.10%
		90%	56.09	50.93	55.60	51.43	69.25	32.98	84.04	13.42	52.59	55.04	96.87%

For ScanQA [3], we use CIDEr [65] and BLEU-4 [54]. SQA3D [50] is measured using exact match accuracy (EM) and its refined version, EM-R [31].

Implementation Details. To validate Fast3D, we apply it to Chat-Scene [29] using the provided checkpoint. The base language model for this 3D MLLM is Vicuna-7B [66]. Under the default setting, Chat-Scene utilizes 300 object-centric visual tokens. Our experimental setup involves training a lightweight GAP network with a transformer-based encoder-decoder architecture, containing 159M total parameters. The GAP network undergoes unified training on combined datasets generated from all five benchmarks. We set the hidden dimension to 768 and use 12 attention heads for all the transformer layers. The language encoder is a three-layer transformer initialized from BERT [19], and the cross-modal decoder contains four layers. The hyper-parameter in the loss function Eq (6) is set to $\lambda = 0.02$. We train the model with a batch size of 64 and a learning rate of 0.0008 using cosine decay scheduling for 50 epochs. The AdamW algorithm [49] is employed in the optimization.

4.2 Experimental Results

Effectiveness of Global Attention Maps. We first investigate the superiority of aggregating attention maps from all layers of the target 3D MLLM. We experiment using different sources to guide visual token pruning. All experiments are conducted based on Chat-Scene model, consisting of 32 layers. We prune 95% visual tokens at the 2-nd layer without the sample-adaptive pruning mechanism, achieving average pruning ratio of 90%.

The results shown in Table 2 indicate that using the global attention maps aggregated from all layers outperforms using partial attention maps from specific layers, such as FastV [9]. Moreover, the average performance consistently improves when the number of aggregated layers increases. This demonstrates that leveraging attention maps from multiple layers helps accurately retain essential visual tokens. Notably, using predicted attention maps from our GAP network achieves performance comparable to the global oracle of the target model, highlighting its effectiveness.

Table 2: Performance with attention maps from different sources. The visual token pruning ratio is set to 90% for all experiments. Predicting attention maps via the GAP network achieves performance comparable to the global oracle of the target model.

attention map source		ScanRefer	Scan2Cap	SQA3D	score ratio
Target Oracle	two layers (FastV [9])	3.23	21.88	50.76	52.26%
	10% layers	8.59	23.49	51.52	57.75%
	30% layers	32.04	29.60	52.02	79.22%
	50% layers	47.70	30.85	53.37	91.53%
	70% layers	51.36	32.11	54.62	95.86%
	all layers (global)	52.72	33.45	55.10	98.28%
GAP Network (ours)		50.93	32.98	55.04	96.63%

Comparing GAP with Previous Methods. To validate the effectiveness of our GAP without the sample-adaptive pruning strategy, we present comparison results in Table 1 with two representative visual token compression methods (*i.e.*, ToMe [4] and FastV [9]) and the random pruning, across different average visual token pruning ratios. For all methods, we apply object-centric pruning, treating each visual token triplet in the 3D MLLM as an integral unit, and adopt fixed pruning ratio from an intermediate layer onward. For our method, FastV [9] and the random pruning, we prune 70%, 80% and 95% visual tokens at the 16-th, 6-th, and 2-nd layer, achieving average pruning ratios of 35%, 65%, and 90%, respectively. ToMe [4] performs token merging prior to the language model, with the merging ratio adjusted to achieve similar average pruning ratios.

In dense captioning and visual question answering tasks, such as Scan2Cap [14], ScanQA [3], and SQA3D [50], when the token pruning ratio is relatively low (*e.g.*, 35%), all methods, even random pruning, exhibit performance comparable to the original model. This indicates significant visual token redundancy in object-centric 3D MLLMs, highlighting the importance of visual token pruning.

When the token pruning ratio is increased to 65%, the performance of ToMe and FastV starts to drop, particularly in visual grounding tasks, including ScanRefer [7] and Multi3DRefer [79],

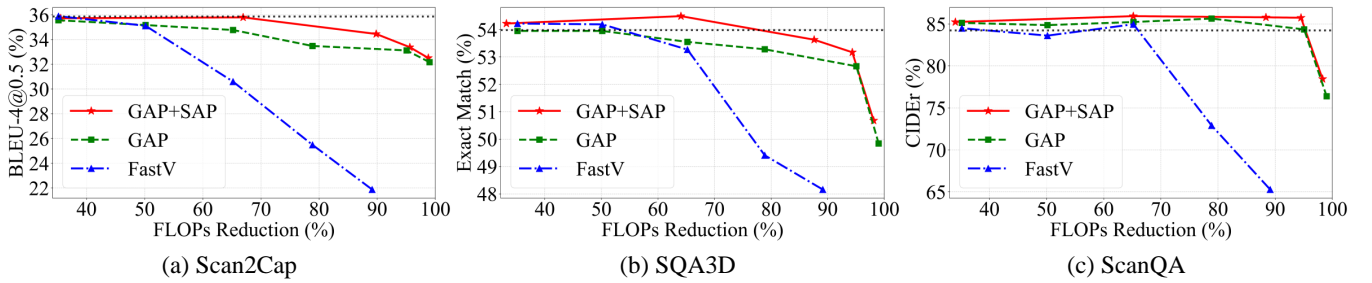


Figure 3: Performance-efficiency trade-off curves of Fast3D (GAP + SAP). The x-axis stands for the theoretical FLOPs reduction ratio under different configurations. The y-axis stands for performance under different settings.

as well as the dense captioning task. These tasks require methods to accurately retain instruction- and answer-related visual tokens to understand 3D scene details. This performance decline shows that ToMe and FastV can not accurately retain essential tokens. In contrast, our method maintains competitive performance across all tasks.

With a visual token pruning ratio of 90%, FastV and ToMe collapse across all tasks, exhibiting performance similar to random pruning, as critical visual tokens are lost due to inaccurate token importance estimation. In this challenging scenario, our method experiences only a marginal performance drop compared to other methods, achieving over 96.8% of the original Chat-Scene’s performance. This validates the superiority of our GAP, which successfully preserves the tokens most relevant to a correct answer, thanks to the global attention maps predicted from the GAP network.

GAP with SAP Towards Improved Efficiency. We further validate the superiority of our Fast3D by incorporating both GAP and SAP mechanisms. The performance-efficiency trade-off curves for varying token pruning ratios across multiple benchmarks are illustrated in Figure 3. We report the overall performance alongside the corresponding theoretical FLOPs reduction ratios related to visual tokens. As detailed in Section 3.3, for each predefined computational budget, we search the optimal pruning strategy on validation samples and perform sample-adaptive pruning on test data based on the derived policy. Note that the additional computational overhead introduced by the GAP network accounts for merely 0.1% of the target model’s FLOPs related to visual tokens, rendering it negligible.

It can be observed that, at lower FLOPs reduction ratios, all methods maintain performance comparable to the original model. However, as the pruning ratio increases, our method GAP without SAP outperforms FastV by significant margins. Furthermore, the proposed SAP enables GAP to sustain performance without any degradation even at higher FLOPs reduction ratios. For instance, on Scan2Cap, the maximum reduction ratio at which performance remains competitive to the original model increases from 40% to over 65%, while on SQA3D, it rises from 50% to approximately 80%. These results demonstrate SAP’s effectiveness in dynamically adjusting layer-wise token budgets based on input complexity, thereby achieving a better balance between overall performance and efficiency.

In summary, our Fast3D provides superior advantages for visual token pruning in 3D MLLMs.

Table 3: Performance of aggregating different attention maps as the GAP network’s training target.

training target	ScanRefer	Scan2Cap	SQA3D	score ratio
\mathbf{a}_{self}	29.34	27.37	51.76	75.21%
$\mathbf{a}_{\text{prompt}}$	42.14	30.16	52.32	86.60%
\mathbf{a}_{text}	46.11	31.25	52.74	90.48%
$\mathbf{a}_{\text{self}} + \mathbf{a}_{\text{prompt}}$	44.68	31.85	54.37	91.05%
$\mathbf{a}_{\text{prompt}} + \mathbf{a}_{\text{text}}$	49.47	32.75	54.49	95.12%
$\mathbf{a}_{\text{self}} + \mathbf{a}_{\text{prompt}} + \mathbf{a}_{\text{text}}$	50.93	32.98	55.04	96.63%

4.3 Ablation Studies

Key Attention Maps Aggregated as Target. Our GAP network adopts aggregated multi-source attention scores as the training target, systematically integrating visual token self-attention \mathbf{a}_{self} , cross-modal attention with textual prompts $\mathbf{a}_{\text{prompt}}$ and generated text tokens \mathbf{a}_{text} . We ablate this design choice without SAP in Table 3. It can be observed that when using only a single attention map, cross-modal attention mechanisms, $\mathbf{a}_{\text{prompt}}$ and \mathbf{a}_{text} , outperform uni-modal self-attention \mathbf{a}_{self} , confirming the value of modality interaction. Furthermore, systematic integration of dual or triple attention maps yields consistent performance improvements, indicating complementary information across different attention maps. These findings validate that multi-source attention aggregation provides comprehensive visual token characterization through the combination of intra- and cross-modal relationships.

Different Embeddings used in GAP Network. We further investigate the effectiveness of different embeddings used in the embedding early fusion of our GAP network, including object identifiers, 3D and 2D semantic embeddings, and spatial location features. As shown in Table 4, object identifiers \mathbf{E}^o emerge as indispensable components for the Scan2Cap dense captioning task, primarily due to their pivotal role in accurate object referring. 2D semantic features \mathbf{E}^v derived from multi-view images yields better performance than using 3D features \mathbf{E}^p , suggesting that the pre-trained 2D encoder better capture discriminative object characteristics. Combining both 3D and 2D semantic embeddings achieve notable performance gain, validating the complementary nature of 3D and 2D information. Explicit integration of spatial location features \mathbf{I} can further boost performance. These results demonstrate that fusing heterogeneous embeddings – spanning identifier, semantic, and spatial domains – provides comprehensive information for precise visual token importance estimation.

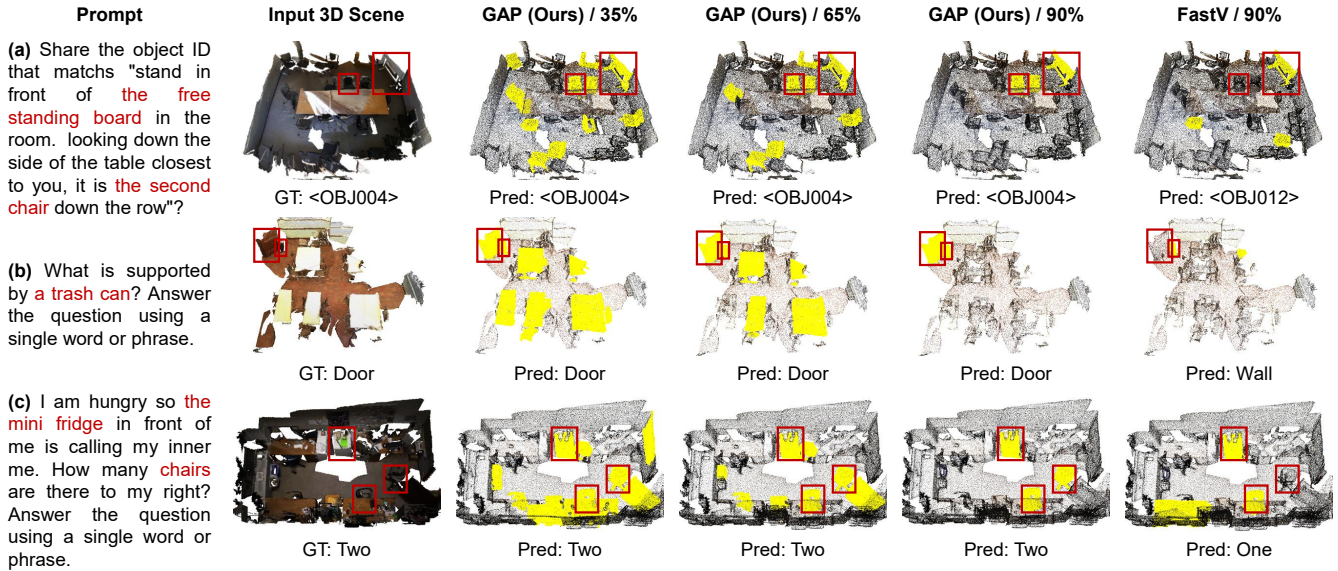


Figure 4: Visualization of GAP under different visual token pruning ratios. Object-centric visual tokens are pruned by 70%, 80%, and 95% at the 16th, 6th, and 2nd layers of Chat-Scene, which comprises 32 layers. This results in average pruning ratios of 35%, 65%, and 90%, respectively. Retained objects are marked in yellow. Red boxes highlight key objects referenced in prompts.

Table 4: Performance of using different input embeddings in the GAP network under 90% average pruning ratio.

used embeddings	ScanRefer	Scan2Cap	SQA3D	score ratio
$E^p + E^v$	48.59	20.28	54.15	82.75%
$E^o + E^p$	46.93	29.70	53.34	89.94%
$E^o + E^v$	47.67	30.56	53.57	91.36%
$E^o + E^p + E^v$	49.82	32.17	54.53	94.84%
$E^o + E^p + E^v + I$	50.93	32.98	55.04	96.63%

Impact of Multi-Objective Optimization. We further investigate the effects of using different loss functions to train our GAP network. While the KL divergence loss \mathcal{L}_{KL} focus on absolute attention distribution matching, our proposed rank consistency loss \mathcal{L}_{rank} emphasizes the relative ordering similarity of attention scores, making it more effective for downstream visual token pruning tasks where relative importance ranking determines preservation decisions. As shown in Table 5, although standalone KL divergence optimization yields competitive results, its combination with rank consistency loss produces significant improvements, validating the effectiveness of multi-objective optimization.

4.4 Visualization Results

To provide a deeper understanding of our GAP, we visualize the token pruning results in Figure 4. Specifically, we present three representative examples from the ScanRefer, ScanQA, and SQA3D benchmarks. These results show that our GAP network consistently retains critical visual tokens essential for various 3D vision-language tasks across varying pruning ratios, demonstrating robust adaptability. Moreover, the network tends to retain core objects explicitly referenced in linguistic prompts (e.g., "board", "chair", "trash can", and "fridge"), showing strong grounding capability to

Table 5: Performance of using different loss functions to train the GAP network.

loss function	ScanRefer	Scan2Cap	SQA3D	score ratio
\mathcal{L}_{KL}	50.43	31.91	54.47	94.97%
$\mathcal{L}_{KL} + \lambda \mathcal{L}_{rank}$	50.93	32.98	55.04	96.63%

identify target objects. We also present the visual token pruning and answers from FastV [9]. Our analysis reveals that FastV only preserves partial tokens relevant to the given instructions and struggles to retain them accurately in 3D scenes. Consequently, this limitation impairs the model's ability to perceive key objects, leading to inaccurate predictions for complex spatial reasoning tasks.

5 Conclusion

In this paper, we explore visual token pruning for scene-level 3D MLLMs. Our findings reveal that token redundancy persists in object-centric representations and global attention remains an effective pruning signal in 3D domains. Based on these insights, we propose Fast3D, a plug-and-play visual token pruning framework tailored for 3D MLLMs with two key components. First, our Global Attention Prediction (GAP) mechanism employs a lightweight neural network to approximate the aggregated attention map from all layers of the target model, enabling efficient token importance estimation for precise pruning guidance. Second, the Sample-Adaptive visual token Pruning (SAP) strategy dynamically adjusts layer-wise pruning ratios based on input complexity, yielding improved overall accuracy-efficiency tradeoffs. Both components operate without modifying the target model's parameters. Experiments on five benchmarks validate the effectiveness of Fast3D, particularly under high visual token pruning ratios.

References

- [1] Josh Achiam, Steven Adler, Sandhini Agarwal, Lama Ahmad, Ilge Akkaya, Florencia Leoni Aleman, Diogo Almeida, Janko Altenschmidt, Sam Altman, Shyamal Anadkat, et al. 2023. Gpt-4 technical report. *arXiv preprint arXiv:2303.08774* (2023).
- [2] Dosovitskiy Alexey. 2020. An image is worth 16x16 words: Transformers for image recognition at scale. *arXiv preprint arXiv:2010.11929* (2020).
- [3] Daichi Azuma, Taiki Miyaniishi, Shuhei Kurita, and Motoaki Kawanabe. 2022. Scanqa: 3d question answering for spatial scene understanding. In *proceedings of the IEEE/CVF conference on computer vision and pattern recognition*. 19129–19139.
- [4] Daniel Bolya, Cheng-Yang Fu, Xiaoliang Dai, Peizhao Zhang, Christoph Feichtenhofer, and Judy Hoffman. 2022. Token merging: Your vit but faster. *arXiv preprint arXiv:2210.09461* (2022).
- [5] Jianjian Cao, Peng Ye, Shengze Li, Chong Yu, Yansong Tang, Jiwen Lu, and Tao Chen. 2024. MADTP: Multimodal Alignment-Guided Dynamic Token Pruning for Accelerating Vision-Language Transformer. In *Proceedings of the IEEE/CVF Conference on Computer Vision and Pattern Recognition*. 15710–15719.
- [6] Junbum Cha, Wooyoung Kang, Jonghwan Mun, and Byungseok Roh. 2024. Honeybee: Locality-enhanced projector for multimodal llm. In *Proceedings of the IEEE/CVF Conference on Computer Vision and Pattern Recognition*. 13817–13827.
- [7] Dave Zhenyu Chen, Angel X Chang, and Matthias Nießner. 2020. Scanrefer: 3d object localization in rgb-d scans using natural language. In *European conference on computer vision*. Springer, 202–221.
- [8] Jieneng Chen, Luoxin Ye, Ju He, Zhao-Yang Wang, Daniel Khashabi, and Alan Yuille. 2024. Llavolta: Efficient multi-modal models via stage-wise visual context compression. *arXiv preprint arXiv:2406.20092* (2024).
- [9] Liang Chen, Haozhe Zhao, Tianyu Liu, Shuai Bai, Junyang Lin, Chang Zhou, and Baobao Chang. 2025. An image is worth 1/2 tokens after layer 2: Plug-and-play inference acceleration for large vision-language models. In *European Conference on Computer Vision*. Springer, 19–35.
- [10] Mengzhao Chen, Wenqi Shao, Peng Xu, Mingbao Lin, Kaipeng Zhang, Fei Chao, Rongrong Ji, Yu Qiao, and Ping Luo. 2023. Diffrate: Differentiable compression rate for efficient vision transformers. In *Proceedings of the IEEE/CVF International Conference on Computer Vision*. 17164–17174.
- [11] Sijin Chen, Xin Chen, Chi Zhang, Mingsheng Li, Gang Yu, Hao Fei, Hongyuan Zhu, Jiayuan Fan, and Tao Chen. 2024. LL3DA: Visual Interactive Instruction Tuning for Omni-3D Understanding Reasoning and Planning. In *Proceedings of the IEEE/CVF Conference on Computer Vision and Pattern Recognition*. 26428–26438.
- [12] Shizhe Chen, Pierre-Louis Guhur, Makarand Tapaswi, Cordelia Schmid, and Ivan Laptev. 2022. Language conditioned spatial relation reasoning for 3d object grounding. *Advances in neural information processing systems* 35 (2022), 20522–20535.
- [13] Yilun Chen, Shuai Yang, Haifeng Huang, Tai Wang, Ruiyuan Lyu, Runsen Xu, Dahua Lin, and Jiangmiao Pang. 2024. Grounded 3D-LLM with Referent Tokens. *arXiv preprint arXiv:2405.10370* (2024).
- [14] Zhenyu Chen, Ali Gholami, Matthias Nießner, and Angel X Chang. 2021. Scan2cap: Context-aware dense captioning in rgb-d scans. In *Proceedings of the IEEE/CVF conference on computer vision and pattern recognition*. 3193–3203.
- [15] Wei-Lin Chiang, Zhuohan Li, Zi Lin, Ying Sheng, Zhanghao Wu, Hao Zhang, Lianmin Zheng, Siyuan Zhuang, Yonghao Zhuang, Joseph E Gonzalez, et al. 2023. Vicuna: An open-source chatbot impressing gpt-4 with 90%* chatgpt quality. See <https://vicuna.lmsys.org> (accessed 14 April 2023) 2, 3 (2023), 6.
- [16] Hengshuo Chu, Xiang Deng, Qi Lv, Xiaoyang Chen, Yinchuan Li, Jianye HAO, and Liqiang Nie. 2025. 3D-AffordanceLLM: Harnessing Large Language Models for Open-Vocabulary Affordance Detection in 3D Worlds. In *The Thirteenth International Conference on Learning Representations*. <https://openreview.net/forum?id=GThTiuXgDC>
- [17] Xiangxiang Chu, Limeng Qiao, Xinyang Lin, Shuang Xu, Yang Yang, Yiming Hu, Fei Wei, Xinyu Zhang, Bo Zhang, Xiaolin Wei, et al. 2023. Mobilevlm: A fast, strong and open vision language assistant for mobile devices. *arXiv preprint arXiv:2312.16886* (2023).
- [18] Xiangxiang Chu, Limeng Qiao, Xinyu Zhang, Shuang Xu, Fei Wei, Yang Yang, Xiaofei Sun, Yiming Hu, Xinyang Lin, Bo Zhang, et al. 2024. Mobilevlm v2: Faster and stronger baseline for vision language model. *arXiv preprint arXiv:2402.03766* (2024).
- [19] Jacob Devlin, Ming-Wei Chang, Kenton Lee, and Kristina Toutanova. 2019. Bert: Pre-training of deep bidirectional transformers for language understanding. In *Proceedings of the 2019 conference of the North American chapter of the association for computational linguistics: human language technologies, volume 1 (long and short papers)*. 4171–4186.
- [20] Mohsen Fayyaz, Soroush Abbasi Koohpayegani, Farnoush Rezaei Jafari, Sunando Sengupta, Hamid Reza Vaezi Joze, Eric Sommerlade, Hamed Pirsiavash, and Jürgen Gall. 2022. Adaptive token sampling for efficient vision transformers. In *European Conference on Computer Vision*. Springer, 396–414.
- [21] Rao Fu, Jingyu Liu, Xilun Chen, Yixin Nie, and Wenhan Xiong. 2024. Scene-llm: Extending language model for 3d visual understanding and reasoning. *arXiv preprint arXiv:2403.11401* (2024).
- [22] Ziyu Guo, Renrui Zhang, Xiangyang Zhu, Yiwen Tang, Xianzheng Ma, Jiaming Han, Kexin Chen, Peng Gao, Xianzhi Li, Hongsheng Li, et al. 2023. Point-bind & point-llm: Aligning point cloud with multi-modality for 3d understanding, generation, and instruction following. *arXiv preprint arXiv:2309.00615* (2023).
- [23] Jiaming Han, Renrui Zhang, Wenqi Shao, Peng Gao, Peng Xu, Han Xiao, Kaipeng Zhang, Chris Liu, Song Wen, Ziyu Guo, et al. 2023. Imagebind-llm: Multi-modality instruction tuning. *arXiv preprint arXiv:2309.03905* (2023).
- [24] Yizeng Han, Gao Huang, Shiji Song, Le Yang, Honghui Wang, and Yulin Wang. 2021. Dynamic neural networks: A survey. *IEEE Transactions on Pattern Analysis and Machine Intelligence* 44, 11 (2021), 7436–7456.
- [25] Yuhang Han, Xuyang Liu, Pengxiang Ding, Donglin Wang, Honggang Chen, Qingsen Yan, and Siteng Huang. 2024. Rethinking Token Reduction in MLLMs: Towards a Unified Paradigm for Training-Free Acceleration. *arXiv preprint arXiv:2411.17686* (2024).
- [26] Yizeng Han, Zeyu Liu, Zhihang Yuan, Yifan Pu, Chaofei Wang, Shiji Song, and Gao Huang. 2024. Latency-aware Unified Dynamic Networks for Efficient Image Recognition. *IEEE Transactions on Pattern Analysis and Machine Intelligence* (2024).
- [27] Shuting He, Henghui Ding, Xudong Jiang, and Bihan Wen. 2024. Segpoint: Segment any point cloud via large language model. In *European Conference on Computer Vision*. Springer, 349–367.
- [28] Yining Hong, Haoyu Zhen, Peihao Chen, Shuhong Zheng, Yilun Du, Zhenfang Chen, and Chuang Gan. 2023. 3d-llm: Injecting the 3d world into large language models. *Advances in Neural Information Processing Systems* 36 (2023), 20482–20494.
- [29] Haifeng Huang, Yilun Chen, Zehan Wang, Rongjie Huang, Runsen Xu, Tai Wang, Luping Liu, Xize Cheng, Yang Zhao, Jiangmiao Pang, et al. 2024. Chat-scene: Bridging 3d scene and large language models with object identifiers. In *The Thirty-eighth Annual Conference on Neural Information Processing Systems*.
- [30] Haifeng Huang, Zehan Wang, Rongjie Huang, Luping Liu, Xize Cheng, Yang Zhao, Tao Jin, and Zhou Zhao. 2023. Chat-3d v2: Bridging 3d scene and large language models with object identifiers. *arXiv preprint arXiv:2312.08168* (2023).
- [31] Jiangyong Huang, Silong Yong, Xiaojian Ma, Xiongfeng Linghu, Puhao Li, Yan Wang, Qing Li, Song-Chun Zhu, Baoxiong Jia, and Siyuan Huang. 2023. An embodied generalist agent in 3d world. *arXiv preprint arXiv:2311.12871* (2023).
- [32] Kai Huang, Hao Zou, Ye Xi, BoChen Wang, Zhen Xie, and Liang Yu. 2024. IVTP: Instruction-Guided Visual Token Pruning for Large Vision-Language Models. In *European Conference on Computer Vision*. Springer, 214–230.
- [33] Wencan Huang, Daizong Liu, and Wei Hu. 2023. Dense object grounding in 3d scenes. In *Proceedings of the 31st ACM International Conference on Multimedia*. 5017–5026.
- [34] Wencan Huang, Daizong Liu, and Wei Hu. 2024. Advancing 3d object grounding beyond a single 3d scene. In *Proceedings of the 32nd ACM International Conference on Multimedia*. 7995–8004.
- [35] Yutao Jiang, Qiong Wu, Wenhao Lin, Wei Yu, and Yiyi Zhou. 2025. What Kind of Visual Tokens Do We Need? Training-free Visual Token Pruning for Multimodal Large Language Models from the Perspective of Graph. *arXiv preprint arXiv:2501.02268* (2025).
- [36] Chen Ju, Haicheng Wang, Haozhe Cheng, Xu Chen, Zhonghua Zhai, Weilin Huang, Jinsong Lan, Shuai Xiao, and Bo Zheng. 2024. Turbo: Informativity-driven acceleration plug-in for vision-language large models. In *European Conference on Computer Vision*. Springer, 436–455.
- [37] Weitai Kang, Haifeng Huang, Yuzhang Shang, Mubarak Shah, and Yan Yan. 2024. Robin3d: Improving 3d large language model via robust instruction tuning. *arXiv preprint arXiv:2410.00255* (2024).
- [38] Xin Lai, Zhuotao Tian, Yukang Chen, Yanwei Li, Yuhui Yuan, Shu Liu, and Jiaya Jia. 2024. Lisa: Reasoning segmentation via large language model. In *Proceedings of the IEEE/CVF Conference on Computer Vision and Pattern Recognition*. 9579–9589.
- [39] Hongliang Li, Jiaxin Zhang, Wenhui Liao, Dezhi Peng, Kai Ding, and Lianwen Jin. 2025. Beyond Token Compression: A Training-Free Reduction Framework for Efficient Visual Processing in MLLMs. *arXiv preprint arXiv:2501.19036* (2025).
- [40] Wentong Li, Yuqian Yuan, Jian Liu, Dongqi Tang, Song Wang, Jie Qin, Jianke Zhu, and Lei Zhang. 2024. Tokenpacker: Efficient visual projector for multimodal llm. *arXiv preprint arXiv:2407.02392* (2024).
- [41] Yanwei Li, Chengyao Wang, and Jiaya Jia. 2024. Llama-vid: An image is worth 2 tokens in large language models. In *European Conference on Computer Vision*. Springer, 323–340.
- [42] Youwei Liang, Chongjian Ge, Zhan Tong, Yibing Song, Jue Wang, and Pengtao Xie. 2022. Not all patches are what you need: Expediting vision transformers via token reorganizations. *arXiv preprint arXiv:2202.07800* (2022).
- [43] Zhihang Lin, Mingbao Lin, Luxi Lin, and Rongrong Ji. 2024. Boosting Multimodal Large Language Models with Visual Tokens Withdrawal for Rapid Inference. *arXiv preprint arXiv:2405.05803* (2024).
- [44] Daizong Liu and Wei Hu. 2025. Seeing is Not Believing: Adversarial Natural Object Optimization for Hard-Label 3D Scene Attacks. In *Proceedings of the Computer Vision and Pattern Recognition Conference*. 11886–11897.
- [45] Daizong Liu, Yang Liu, Wencan Huang, and Wei Hu. 2024. A survey on text-guided 3D visual grounding: elements, recent advances, and future directions. *arXiv preprint arXiv:2406.05785* (2024).

- [46] Daizong Liu, Mingyu Yang, Xiaoye Qu, Pan Zhou, Yu Cheng, and Wei Hu. 2024. A survey of attacks on large vision-language models: Resources, advances, and future trends. *arXiv preprint arXiv:2407.07403* (2024).
- [47] Daizong Liu, Mingyu Yang, Xiaoye Qu, Pan Zhou, Xiang Fang, Keke Tang, Yao Wan, and Lichao Sun. 2024. Pandora's Box: Towards Building Universal Attackers against Real-World Large Vision-Language Models. In *The Thirty-eighth Annual Conference on Neural Information Processing Systems*.
- [48] Haotian Liu, Chunyuan Li, Qingyang Wu, and Yong Jae Lee. 2024. Visual instruction tuning. *Advances in neural information processing systems* 36 (2024).
- [49] Ilya Loshchilov, Frank Hutter, et al. 2017. Fixing weight decay regularization in adam. *arXiv preprint arXiv:1711.05101* 5 (2017), 5.
- [50] Xiaojian Ma, Silong Yong, Zilong Zheng, Qing Li, Yitao Liang, Song-Chun Zhu, and Siyuan Huang. 2022. Sq3d: Situated question answering in 3d scenes. *arXiv preprint arXiv:2210.07474* (2022).
- [51] Lingchen Meng, Hengduo Li, Bor-Chun Chen, Shiyi Lan, Zuxuan Wu, Yu-Gang Jiang, and Ser-Nam Lim. 2022. Adavit: Adaptive vision transformers for efficient image recognition. In *Proceedings of the IEEE/CVF Conference on Computer Vision and Pattern Recognition*. 12309–12318.
- [52] Lingchen Meng, Jianwei Yang, Rui Tian, Xiyang Dai, Zuxuan Wu, Jianfeng Gao, and Yu-Gang Jiang. 2024. DeepStack: Deeply Stacking Visual Tokens is Surprisingly Simple and Effective for LMMs. *arXiv preprint arXiv:2406.04334* (2024).
- [53] Maxime Oquab, Timothée Darcet, Théo Moutakanni, Huy Vo, Marc Szafraniec, Vasil Khalidov, Pierre Fernandez, Daniel Haziza, Francisco Massa, Alaaeldin El-Nouby, et al. 2023. Dinov2: Learning robust visual features without supervision. *arXiv preprint arXiv:2304.07193* (2023).
- [54] Kishore Papineni, Salim Roukos, Todd Ward, and Wei-Jing Zhu. 2002. Bleu: a method for automatic evaluation of machine translation. In *Proceedings of the 40th annual meeting of the Association for Computational Linguistics*. 311–318.
- [55] Zekun Qi, Runpei Dong, Shaochen Zhang, Haoran Geng, Chunrui Han, Zheng Ge, Li Yi, and Kaisheng Ma. 2024. Shapellm: Universal 3d object understanding for embodied interaction. In *European Conference on Computer Vision*. Springer, 214–238.
- [56] Zhangyang Qi, Ye Fang, Zeyi Sun, Xiaoyang Wu, Tong Wu, Jiaqi Wang, Dahua Lin, and Hengshuang Zhao. 2024. Gpt4point: A unified framework for point-language understanding and generation. In *Proceedings of the IEEE/CVF Conference on Computer Vision and Pattern Recognition*. 26417–26427.
- [57] Zhangyang Qi, Zhixiong Zhang, Ye Fang, Jiaqi Wang, and Hengshuang Zhao. 2025. GPT4Scene: Understand 3D Scenes from Videos with Vision-Language Models. *arXiv preprint arXiv:2501.01428* (2025).
- [58] Yongming Rao, Wenliang Zhao, Benlin Liu, Jiwen Lu, Jie Zhou, and Cho-Jui Hsieh. 2021. Dynamicvit: Efficient vision transformers with dynamic token sparsification. *Advances in neural information processing systems* 34 (2021), 13937–13949.
- [59] Jonas Schult, Francis Engelmann, Alexander Hermans, Or Litany, Siyu Tang, and Bastian Leibe. 2023. Mask3d: Mask transformer for 3d semantic instance segmentation. In *2023 IEEE International Conference on Robotics and Automation (ICRA)*. IEEE, 8216–8223.
- [60] Yuzhang Shang, Mu Cai, Bingxin Xu, Yong Jae Lee, and Yan Yan. 2024. Llva-prunemerge: Adaptive token reduction for efficient large multimodal models. *arXiv preprint arXiv:2403.15388* (2024).
- [61] Dachuan Shi, Chaofan Tao, Anyi Rao, Zhendong Yang, Chun Yuan, and Jiaqi Wang. 2023. Crossget: Cross-guided ensemble of tokens for accelerating vision-language transformers. *arXiv preprint arXiv:2305.17455* (2023).
- [62] Yuan Tang, Xu Han, Xianzhi Li, Qiao Yu, Yixue Hao, Long Hu, and Min Chen. 2024. Minigpt-3d: Efficiently aligning 3d point clouds with large language models using 2d priors. In *Proceedings of the 32nd ACM International Conference on Multimedia*. 6617–6626.
- [63] Hugo Touvron, Thibaut Lavril, Gautier Izacard, Xavier Martinet, Marie-Anne Lachaux, Timothée Lacroix, Baptiste Rozière, Naman Goyal, Eric Hambro, Faisal Azhar, et al. 2023. Llama: Open and efficient foundation language models. *arXiv preprint arXiv:2302.13971* (2023).
- [64] A Vaswani. 2017. Attention is all you need. *Advances in Neural Information Processing Systems* (2017).
- [65] Ramakrishna Vedantam, C Lawrence Zitnick, and Devi Parikh. 2015. Cider: Consensus-based image description evaluation. In *Proceedings of the IEEE conference on computer vision and pattern recognition*. 4566–4575.
- [66] Vicuna. 2023. Vicuna: An Open-Source Chatbot Impressing GPT-4 with 90%* ChatGPT Quality. <https://vicuna.lmsys.org/>.
- [67] Ao Wang, Fengyuan Sun, Hui Chen, Zijia Lin, Jungong Han, and Guiguang Ding. 2024. [CLS] Token Tells Everything Needed for Training-free Efficient MLLMs. *arXiv preprint arXiv:2412.05819* (2024).
- [68] Hongjie Wang, Bhishma Dedhia, and Niraj K Jha. 2024. Zero-TPrune: Zero-shot token pruning through leveraging of the attention graph in pre-trained transformers. In *Proceedings of the IEEE/CVF Conference on Computer Vision and Pattern Recognition*. 16070–16079.
- [69] Zehan Wang, Haifeng Huang, Yang Zhao, Ziang Zhang, Tao Jin, and Zhou Zhao. 2025. Data-Efficiently Learn Large Language Model for Universal 3D Scene Perception. In *Findings of the Association for Computational Linguistics: NAACL 2025*. 313–333.
- [70] Zehan Wang, Haifeng Huang, Yang Zhao, Ziang Zhang, and Zhou Zhao. 2023. Chat-3d: Data-efficiently tuning large language model for universal dialogue of 3d scenes. *arXiv preprint arXiv:2308.08769* (2023).
- [71] Zhanyu Wang, Longyue Wang, Zhen Zhao, Minghao Wu, Chenyang Lyu, Huayang Li, Deng Cai, Luping Zhou, Shuming Shi, and Zhaopeng Tu. 2024. Gpt4video: A unified multimodal large language model for instruction-followed understanding and safety-aware generation. In *Proceedings of the 32nd ACM International Conference on Multimedia*. 3907–3916.
- [72] Runsen Xu, Xiaolong Wang, Tai Wang, Yilun Chen, Jiangmiao Pang, and Dahua Lin. 2024. Pointllm: Empowering large language models to understand point clouds. In *European Conference on Computer Vision*. Springer, 131–147.
- [73] Linli Yao, Lei Li, Shuhui Ren, Lean Wang, Yuanxin Liu, Xu Sun, and Lu Hou. 2024. DeCo: Decoupling Token Compression from Semantic Abstraction in Multimodal Large Language Models. *arXiv preprint arXiv:2405.20985* (2024).
- [74] Weihao Ye, Qiong Wu, Wenhao Lin, and Yiyou Zhou. 2024. Fit and prune: Fast and training-free visual token pruning for multi-modal large language models. *arXiv preprint arXiv:2409.10197* (2024).
- [75] Xubing Ye, Yukang Gan, Xiaoke Huang, Yixiao Ge, Ying Shan, and Yansong Tang. 2024. VoCo-LLaMA: Towards Vision Compression with Large Language Models. *arXiv preprint arXiv:2406.12275* (2024).
- [76] Hanxun Yu, Wentong Li, Song Wang, Junbo Chen, and Jianke Zhu. 2025. Inst3d-lmm: Instance-aware 3d scene understanding with multi-modal instruction tuning. In *Proceedings of the Computer Vision and Pattern Recognition Conference*. 14147–14157.
- [77] Tatiana Zemszkova and Dmitry Yudin. 2024. 3DGraphLLM: Combining Semantic Graphs and Large Language Models for 3D Scene Understanding. *arXiv preprint arXiv:2412.18450* (2024).
- [78] Yuan Zhang, Chun-Kai Fan, Junpeng Ma, Wenzhao Zheng, Tao Huang, Kuan Cheng, Denis Gudovskiy, Tomoyuki Okuno, Yohei Nakata, Kurt Keutzer, et al. 2024. Sparsevlm: Visual token sparsification for efficient vision-language model inference. *arXiv preprint arXiv:2410.04417* (2024).
- [79] Yiming Zhang, ZeMing Gong, and Angel X Chang. 2023. Multi3drefer: Grounding text description to multiple 3d objects. In *Proceedings of the IEEE/CVF International Conference on Computer Vision*. 15225–15236.
- [80] Shiyu Zhao, Zhenting Wang, Felix Juefei-Xu, Xide Xia, Miao Liu, Xiaofang Wang, Mingfu Liang, Ning Zhang, Dimitris N Metaxas, and Licheng Yu. 2024. Accelerating Multimodal Large Language Models by Searching Optimal Vision Token Reduction. *arXiv preprint arXiv:2412.00556* (2024).
- [81] Wangbo Zhao, Yizeng Han, Jiasheng Tang, Zhikai Li, Yibing Song, Kai Wang, Zhangyang Wang, and Yang You. 2024. A Stitch in Time Saves Nine: Small VLM is a Precise Guidance for accelerating Large VLMs. *arXiv preprint arXiv:2412.03324* (2024).
- [82] Wangbo Zhao, Yizeng Han, Jiasheng Tang, Kai Wang, Yibing Song, Gao Huang, Fan Wang, and Yang You. 2024. Dynamic diffusion transformer. *arXiv preprint arXiv:2410.03456* (2024).
- [83] Wangbo Zhao, Jiasheng Tang, Yizeng Han, Yibing Song, Kai Wang, Gao Huang, Fan Wang, and Yang You. 2024. Dynamic tuning towards parameter and inference efficiency for vit adaptation. *arXiv preprint arXiv:2403.11808* (2024).
- [84] Yiwu Zhong, Zhuoming Liu, Yin Li, and Liwei Wang. 2024. Aim: Adaptive inference of multi-modal llms via token merging and pruning. *arXiv preprint arXiv:2412.03248* (2024).
- [85] Junsheng Zhou, Jinsheng Wang, Baorui Ma, Yu-Shen Liu, Tiejun Huang, and Xinlong Wang. 2023. Uni3d: Exploring unified 3d representation at scale. *arXiv preprint arXiv:2310.06773* (2023).
- [86] Deyao Zhu, Jun Chen, Xiaoqian Shen, Xiang Li, and Mohamed Elhoseiny. 2023. Minigpt-4: Enhancing vision-language understanding with advanced large language models. *arXiv preprint arXiv:2304.10592* (2023).
- [87] Jiedong Zhuang, Lu Lu, Ming Dai, Rui Hu, Jian Chen, Qiang Liu, and Haoji Hu. 2024. ST³: Accelerating Multimodal Large Language Model by Spatial-Temporal Visual Token Trimming. *arXiv preprint arXiv:2412.20105* (2024).